Journal of Quality Measurement and Analysis *JQMA* 14(1) 2018, 91-99
Jurnal Pengukuran Kualiti dan Analisis

CONJUGATE HEAT TRANSFER ANALYSIS IN TWO SQUARE ENCLOSURES WITH BOUNDED AND PARTITIONED CONDUCTIVE WALL

(Analisis Pemindahan Haba Konjugat dalam Dua Kurungan Persegi dengan Batas dan Sekatan Dinding Konduktif)

MARHAMA JELITA[1], SUTOYO[1] & HABIBIS SALEH[2]

ABSTRACT

Conjugate heat transfer in two square enclosures are studied numerically in the present article. Effects of a finite side wall thickness and a finite partition thickness on the fluid flow pattern, and heat transfer rate are studied comprehensively. An iterative finite difference procedure is employed to solve the governing equations. The study is performed for different wall thickness and thermal conductivity ratio. The extreme size of the wall thickness for both enclosure is obtained under specific conditions. The maximum ratio of the heat transfer rate is achieved by adjusting the solid size to proportional to the thermal conductivity ratio.

Keywords: conjugate heat transfer; natural convection; Finite difference method

ABSTRAK

Pemindahan haba konjugat dalam dua kurungan persegi dikaji secara berangka dalam makalah ini. Kesan ketebalan terhingga dinding sisi dan ketebalan terhingga sekatan pada corak aliran bendalir dan kadar pemindahan haba diselidiki secara menyeluruh. Tatacara lelaran beza terhingga dibuat untuk menyelesaikan persamaan menakluk. Kajian dilakukan untuk pelbagai ketebalan dinding dan nisbah kekonduksian terma. Ukuran ketebalan dinding ekstrim untuk kedua-dua kurungan diperoleh tertakluk kepada syarat-syarat khas. Nisbah maksimum kadar pemindahan haba dicapai dengan menyesuaikan ukuran pepejal supaya setanding dengan nisbah kekonduksian terma.

Kata kunci: pemindahan haba konjugat; olakan semula jadi; kaedah beza terhingga

1. Introduction

Thermally driven flow and heat transfer in differentially heated enclosures has received considerable attention over the past few decades, largely due to potential application availability. Comprehensive theoretically or experimentally studies on natural convection have been conducted by many authors. The topic of these studies is mostly enclosure surrounded by walls with zero thickness. In some situations, the conductivities of the enclosure walls and the fluid inside are comparable and the wall thickness is finite. These pair of conduction-convection heat transfer is called as conjugate heat transfer.

Conjugate heat transfer in a rectangular enclosure bounded by solid walls was firstly examined by Kim and Viskanta (1984). Their results indicates that the solid decrease the average temperature differences across the enclosure, fractionally suppress the fluid circulation and reduce the thermal performance. A natural convection from the side heating of vertical square enclosure with two finite thickness horizontal walls was studied by Mobedi (2008). Misra and Sarkar (1997) performed a numerical study on conjugate heat transfer in a square enclosure with a finite wall installed on the right surface. Zhang *et al.* (2011) studied effect of

pulsating the wall temperature and the orientation angle on the conjugate heat transfer. Recently, Jamesahar *et al.* (2016) studied unsteady interaction of the fluid and solid structure in a square cavity divided into two triangles using a flexible thermal conductive membrane.

Conjugate heat transfer in a rectangular enclosure with a vertical partition and filled with air was firstly studied by Tong and Gerner (1986). They found that partitioning is an effective method of reducing heat transfer and the maximum reduction in heat transfer occurs when the partition was placed midway between the vertical walls. The heat transfer rate was found considerably attenuated in a partitioned enclosure in comparing with that for non-partitioned enclosure as reported by Ho and Yih (1987). Nishimura *et al.* (1988) studied numerically and experimentally enclosures with multiple vertical partitions and showed that the Nusselt number is inversely proportional to the number of partitions. Kahveci (2007) used differential quadrature method to solve the problem and found the average Nusselt number increases with decreasing of thermal resistance of the partition and the partition thickness has little effect on heat transfer. Oztop *et al.* (2009) studied a vertically divided square enclosure by a solid partition into air and water regions and found that filling of fluid into chests is important for obtaining maximum heat transfer and energy saving. Zhang *et al.* (2016) addressed on the optimization of heat transfer rate by varying the partitions location, partitions size and thermal conductivity ratio. Hu *et al.* (2016) investigated two configurations of obstacles number using numerical and analytical methods and they concluded the average Nusselt number is an increasing function of Rayleigh number and conductivity ratio. A thick walled open cavity filled with a nanofluid was investigated by Bondareva *et al.* (2017).

To the best of our knowledge, no report has been obtained for systematical comparison of enclosure bounded by conductive solid walls and ones partitioned with a solid conduction body. Essentially, controlling the heat transfer in the enclosure use a solid body partition or installing thick solid walls. The aim of this work is to solve numerically and give a systematical comparison of enclosure bounded by conductive walls and ones partitioned with a conduction wall. Both enclosures were maintained equivalent fluid volumes by the same volume ratio magnitude.

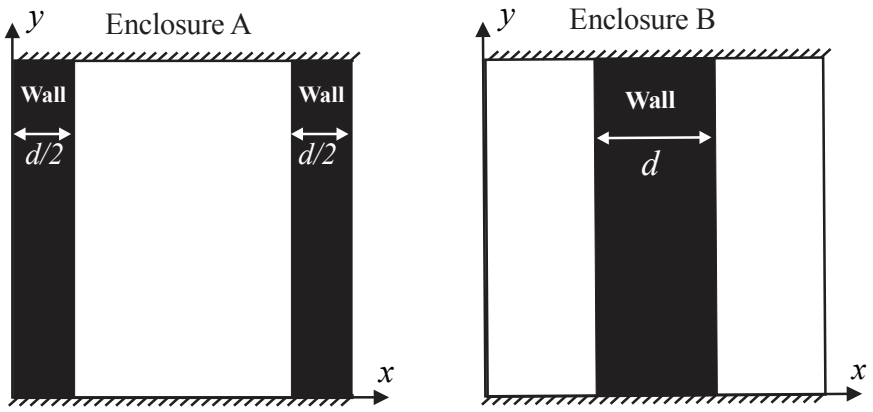

Figure 1: Schematic representation of the model A and B

2. Mathematical Formulation

A schematic diagram of two square enclosures with differentially heated is shown in Figure 1. Enclosure A is attached by conductive walls. The enclosure B is partitioned or divided by a

solid wall. When the wall approaches zero, both enclosures evolve into fluid-filled enclosure, while the wall approach the enclosure size, both enclosures are filled with solid block.

The governing equation base on conservation laws of mass, momentum and energy with appropriate rheological models and equations. The Boussinesq approximation is assumed to be valid. The steady conjugate heat transfer equations can be written as:

$$\frac{\partial u}{\partial x}+\frac{\partial v}{\partial y}=0, \tag{1}$$

$$u\frac{\partial u}{\partial x}+v\frac{\partial u}{\partial y}=-\frac{1}{\rho}\frac{\partial p}{\partial x}+\nu\left(\frac{\partial^2 u}{\partial x^2}+\frac{\partial^2 u}{\partial y^2}\right), \tag{2}$$

$$u\frac{\partial v}{\partial x}+v\frac{\partial v}{\partial y}=-\frac{1}{\rho}\frac{\partial p}{\partial y}+\nu\left(\frac{\partial^2 v}{\partial x^2}+\frac{\partial^2 v}{\partial y^2}\right)+g\beta\left(T_f-T_c\right), \tag{3}$$

$$u\frac{\partial T_f}{\partial x}+v\frac{\partial T_f}{\partial y}=\alpha\left(\frac{\partial^2 T_f}{\partial x^2}+\frac{\partial^2 T_f}{\partial y^2}\right), \tag{4}$$

and the energy equation for the solid walls are:

$$\frac{\partial^2 T_w}{\partial x^2}+\frac{\partial^2 T_w}{\partial y^2}=0, \tag{5}$$

where the subscripts f and w stand for the fluid and the wall respectively. No-slip condition is assumed at all the solid-fluid interfaces. Using the following non-dimensional variables:

$$X=\frac{x}{\ell},Y=\frac{y}{\ell},U=\frac{u\ell}{\alpha},V=\frac{v\ell}{\alpha},\Theta_f=\frac{T_f-T_c}{T_h-T_c}, \tag{6}$$

$$\Theta_w=\frac{T_w-T_c}{T_h-T_c},P=\frac{p\ell^2}{p\alpha^2},Pr=\frac{\nu}{\alpha},Ra=\frac{g\beta(T_h-T_c)\ell^3 Pr}{\nu^2}.$$

The partial differential equations given above are in terms of the so-called primitive variables, i.e. u, v, p and T. The solution procedure discussed in this work is based on equations involving the stream function, ψ,the vorticity, ω, and the temperature, T, as variables which are defined as $u=\partial\psi/\partial y, v=-\partial\psi/\partial x$ and $\omega=(\partial v/\partial x)-(\partial u/\partial y)$. Eliminating the pressure between the two momentum equations, writing in the stream function, vorticity and temperature formulation, performing nondimesionalization, then Eqs. (1) – (5) become:

$$\frac{\partial^2\psi}{\partial X^2}+\frac{\partial^2\psi}{\partial Y^2}=-\Omega, \tag{7}$$

$$\frac{\partial^2\Omega}{\partial X^2}+\frac{\partial^2\Omega}{\partial Y^2}=\frac{1}{Pr}\left(\frac{\partial\psi}{\partial Y}\frac{\partial\Omega}{\partial X}-\frac{\partial\psi}{\partial X}\frac{\partial\Omega}{\partial Y}\right)+Ra\ \frac{\partial\Theta_f}{\partial X}, \tag{8}$$

$$\frac{\partial^2\Theta_f}{\partial X^2}+\frac{\partial^2\Theta_f}{\partial Y^2}=\frac{\partial\psi}{\partial Y}\frac{\partial\Theta_f}{\partial X}-\frac{\partial\psi}{\partial X}\frac{\partial\Theta_f}{\partial Y}, \tag{9}$$

$$\frac{\partial^2\Theta_w}{\partial X^2}+\frac{\partial^2\Theta_w}{\partial Y^2}=0. \tag{10}$$

The values of the nondimensional velocity are zero in the wall regions and on the solid-fluid surfaces. The boundary conditions for the non-dimensional temperatures are:

$$\Theta(0,Y)=1;\Theta(1,Y)=0, \tag{11}$$

$$\frac{\partial\Theta(X,0)}{\partial Y}=\frac{\partial\Theta(X,1)}{\partial Y}=0. \tag{12}$$

Continuity of the heat flux at the solid-fluid surfaces:

$$\frac{\partial\Theta_f}{\partial Y}=K_r\frac{\partial\Theta_w}{\partial Y}, \tag{13}$$

where $K_r=k_w/k_f$ is the thermal conductivity ratio. At the same time, continuity of the temperature at the solid-fluid surface for the both enclosure is represented by

$$\Theta_f=\Theta_w. \tag{14}$$

The heat transfer rate across the enclosure is an important parameter in heat transfer applications. The total heat transfer rate in terms of the average Nusselt number, $(\overline{Nu})$ at the solid-fluid interfaces is defined as:

$$\overline{Nu}=\int_0^1-\frac{\partial\Theta}{\partial X}dY. \tag{15}$$

3. Numerical Method and Validation

An iterative finite difference procedure is employed to solve Eqs. (7) – (10) subject to the boundary conditions Eqs. (11) – (14). The numerical solution will be preceded by giving the finite difference equation (FDE) of the stream function Eq. (7) to energy equation for the wall Eq. (10) for the bounded enclosure and the partitioned enclosure. The FDE of the stream function written in the Gaussian SOR formulation is:

$$\begin{aligned}\psi_{i,j}^{k+1} \;=\; & \psi_{i,j}^{k}+\frac{\lambda_r}{2(1+B^2)}\left[\psi_{i+1,j}^{k}+\psi_{i-1,j}^{k+1}\right]+B^2\left(\psi_{i,j+1}^{k}+\psi_{i,j-1}^{k+1}\right)\\ & -2(1+B^2)\Psi_{i,j}^{k}+(\Delta X)^2\left(S_\psi\right)_{i,j}^{k},\end{aligned} \tag{16}$$

with

$$B = \frac{\Delta X}{\Delta Y}, \qquad \left(S_\psi\right)_{i,j} = -\Omega_{i,j}\,. \tag{17}$$

The FDE of vorticity, energy in the fluid and wall equations could be wrote in the same way. The conditions at the interface boundary are:

$$\begin{aligned}\left(\Theta_f\right)_{i,j}^{k+1} &= \left(\Theta_w\right)_{i,j}^{k},\\ \left(\Theta_w\right)_{i,j}^{k+1} &= \left[\left(\frac{1}{Kr}\right)\left(-\left(\Theta_f\right)_{i,j+2}^{k} + 4\left(\Theta_f\right)_{i,j+1}^{k} - 3\left(\Theta_f\right)_{i,j}^{k}\right) + 4\left(\Theta_w\right)_{i,j-1}^{k}\right.\\ &\qquad \left. - \left(\Theta_w\right)_{i,j-1}^{k}\right]/3\,.\end{aligned} \tag{18}$$

Regular and uniform grid distribution is used for the whole enclosure. The effect of grid resolution was examined in order to select the appropriate grid density; the results indicate that a 110×110 grid can be used in the final computations. The integration of average Nusselt number defined in Eq. (15) is done by using the second order Simpson method. As a qualitative validation, our results for the streamlines and isotherms compare good enough with that obtained by Oztop *et al.* (2009) for enclosure B filled with water and air, $D = 0.1$ and several values of Grashof numbers ($Gr = Ra/\mathrm{Pr}$), (a) $Gr = 10^3$, (b) $Gr = 10^5$and (c) $Gr = 10^6$, see Figure 2. The quantitative data of the $\psi_{\min}$ from Oztop *et al.* (2009) were also integrated in the figure. As seen from the figure, the $\psi_{\min}$ present results show good agreement with the literature. Thus, it is decided that the present code is valid for further calculations.

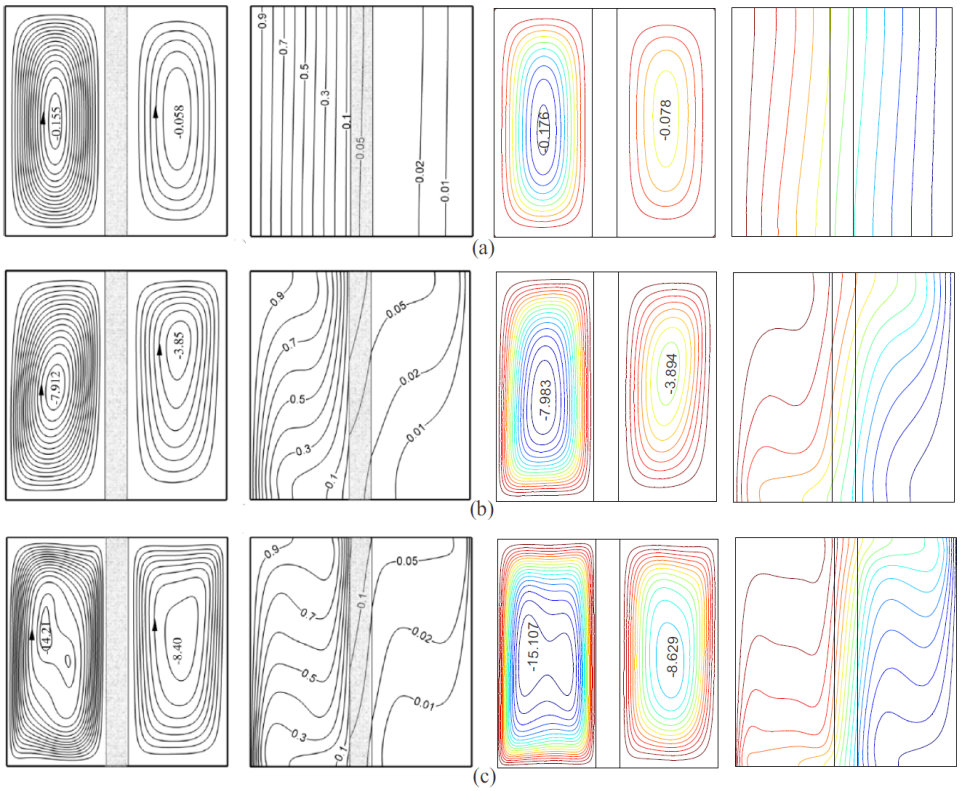

Figure 2: Comparison of the present result (right) against that of literature result (left) for the enclosure B

4. Result and Discussion

The analysis in the undergoing numerical investigation are performed in the following range of the associated dimensionless groups: the wall thickness, $0.0 \leq D \leq 1.0$, the thermal conductivity ratio,$0.1 \leq K_r \leq 10.0$. The Prandtl number is fixed at $Pr = 0.71$ and Rayleigh number is fixed at $Ra = 10^5$.

Figure 3 depicts the effects of the wall thickness for enclosure A and enclosure B on the streamlines for $K_r = 1$. Without solid wall ($D = 0.0$), a skewed and stretched eddy flow is found in the center of the enclosure. The eddy in enclosure A becomes a circled one as wall thickness increasesand later the eddy flow is elongated vertically. The vertically elongated eddy in the hot portion of enclosure B is found in the lower part of the enclosure, while the eddy in the cold portion is found in the upper part of the enclosure. The streamlines in enclosure A and B generally show that as the D increases, the fluid circulation strength decreases to a certain extent due to the narrowing of the fluids region. The circulation strength in enclosure A is considerably greater than that in enclosure B for the same wall thickness. This attributes to that the convective flow in enclosure B is blocked by the solid partition. Figure 3 also shows the spatial displacement and changing of cores orientation of the convective cells by varying the solid width. Almost two whirls are formed in the pure natural convection in the enclosure without solid parts. There is more intensive fluid motion in the pure natural case owing to the direct fluid heating of the left layer. It notes that the both enclosure becomes solid body at $D = 1.0$ where no fluid circulation or streamlines inside the body.

Variations of the average Nusselt number of both enclosures with the wall thickness are shown in Figure 4 for different values of K_r. The average Nusselt number ratio of $\overline{Nu}_A$ to $\overline{Nu}_B$ as a function of the wall thickness for different K_r is also integrated in this figure. The $\overline{Nu}$ of both enclosures decreases by increasing the wall thickness for $K_r = 0.1$ and $K_r = 0.5$. However, for $K_r = 2.0$ and $K_r = 10.0$, there exist an extreme wall size D_c below which increasing D decreases $\overline{Nu}_A$ and $\overline{Nu}_B$ and above which increasing D increases the average Nusselt number of both enclosures. The D_c of $\overline{Nu}_A$ was obtained at $D = 0.75$ for $K_r = 2.0$ and $K_r = 10.0$. The D_c of $\overline{Nu}_B$ was obtained at $D = 0.475$ and $D = 0.375$ for $K_r = 2.0$ and $K_r = 10.0$, respectively. Increasing the solid conductivity makes the D_c to occur at a thinner wall thickness. The $\overline{Nu}_A$ is greater than $\overline{Nu}_B$ for any combination of the wall thickness and thermal conductivity ratio. The average Nusselt number ratio reaches its maximum 2.211 at $D = 0.325$ for $K_r = 10.0$. The maximum ratio decreases as K_r decreases and it occurs at a thinner wall thickness i.e. $D = 0.025$. The average ratio collapses into unity as the wall thickness is close to 0.0 or greater than 0.8.

5. Conclusion

In the present numerical simulations, we have studied two categories of morphology, the bounded enclosure and the partitioned enclosure. The dimensionless forms of the partial differential equation were solved using the finite difference method (FDM). The main conclusions of the present analysis are as follows:

(1) An extreme size of the wall thickness is exist at low conductivities for the both enclosure, below which the size increases, the average Nusselt number decreases and above which the size increases, the average Nusselt number increases. The extreme thickness of the bounded enclosure is greater than the extreme thickness of the partitioned enclosure

(2) The global amount of heat transfer of the bounded enclosure could be twice of the partitioned enclosure under specific condition.

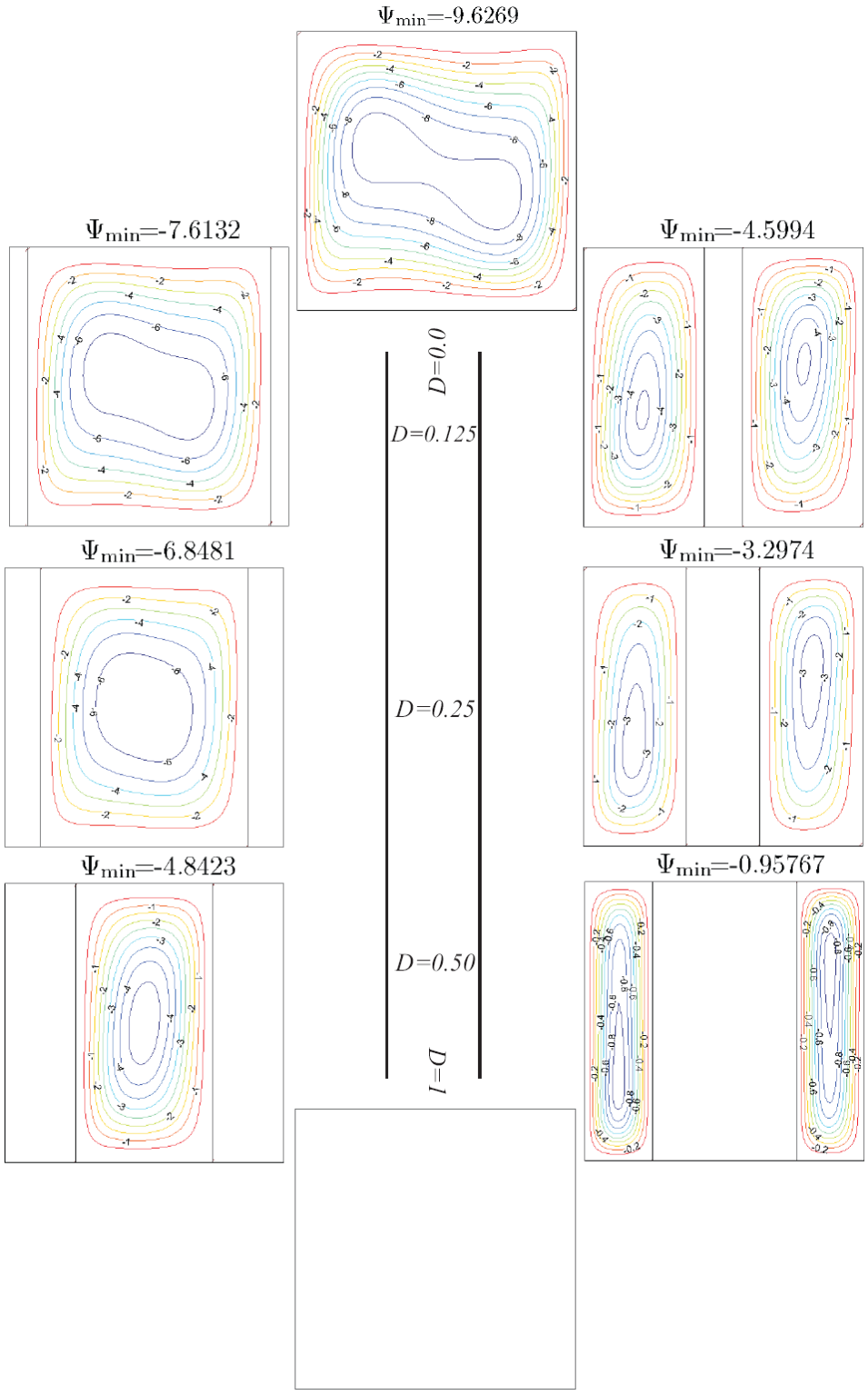

Figure 3: Streamlines evolutions by varying wall thickness at $K_r = 1.0$

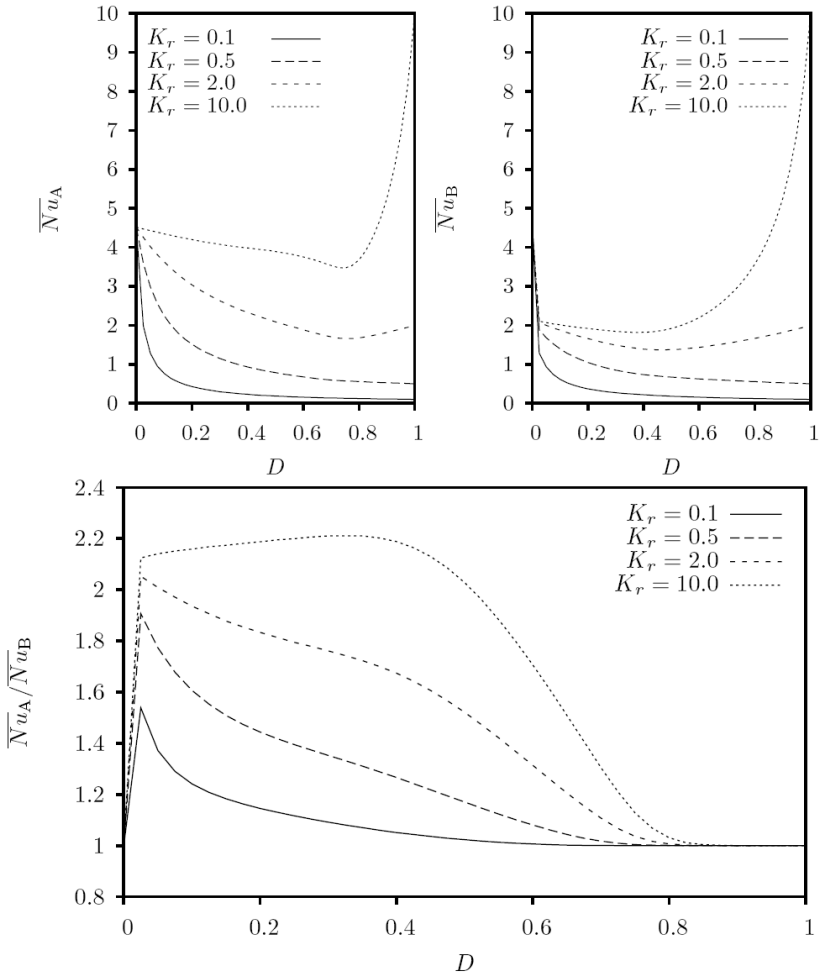

Figure 4: Variation of $\overline{Nu_A}$, $\overline{Nu_B}$ (top) and their ratio (bottom) with D for different K_r

(3) The maximum ratio of the heat transfer rate by adjusting the solid size is proportional to the thermal conductivity ratio.

The results of this study can be used in the design of an effective cooling in electronic system or heat preservation in building system to help ensure effective, safe, comfortable operational conditions and material saving purpose.

References

Alsabery A., Chamkha A., Saleh H. & Hashim I. 2016. Heatline visualization of conjugate natural convection in a square cavity filled with nanofluid with sinusoidal temperature variations on both horizontal walls. *International Journal Heat Mass Transfer* **100**: 835–850.

Bondareva N.S., Sheremet M.A., Oztop H.F. & Abu-Hamdeh N. 2017. Heatline visualization of natural convection in a thick walled open cavity filled with a nanofluid. *International Journal Heat Mass Transfer* **109**: 175–186.

Ho C., Yih Y. 1987. Conjugate natural heat transfer in an air-filled rectangular cavity. *International Comm. Heat Mass Transfer* **14**: 91–100.

Hu J.T., Ren X.H., Liu D., Zhao F.Y. & Wang H.Q. 2016. Conjugate natural convection inside a vertical enclosure with solid obstacles of unique volume and multiple morphologies. *International Journal Heat Mass Transfer* **95**: 1096–1114.

Jamesahar E., Ghalambaz M. & Chamkha A.J. 2016. Fluid–solid interaction in natural convection heat transfer in a square cavity with a perfectly thermal-conductive flexible diagonal partition. *International Journal Heat Mass Transfer* **100**: 303–319.

Kahveci K. 2007. A differential quadrature solution of natural convection in an enclosure with a finite-thickness partition. *Numeric Heat Transfer Part A* **52**:1009–1026.
Kim D.M. & Viskanta R. 1984. Study of the effects of wall conductance on natural convection in differently oriented square cavities. *Journal Fluid Mechanics* **144**: 153–176.
Misra D. & Sarkar A. 1997. Finite element analysis of conjugate natural convection in a square enclosure with a conducting vertical wall. *Computer Methods in Applied Mechanics and Engineering* **141**: 205–219.
Mobedi M. 2008. Conjugate natural convection in a square cavity with finite thickness horizontal walls. *International Comm. Heat Mass Transfer* **35**: 503–513.
Nishimura T., Shiraishi M., Nagasawa F. & Kawamura Y. 1988. Natural convection heat transfer in enclosures with multiple vertical partitions. *International Journal Heat Mass Transfer* **31**:1679–1686.
Oztop H.F., Varol Y. & Koca A. 2009. Natural convection in a vertically divided square enclosure by a solid partition into air and water regions. International Journal Heat Mass Transfer **52**: 5909–5921.
Tong T. & Gerner F. 1986. Natural convection in partitioned air-filled rectangular enclosures. *International Comm. Heat Mass Transfer* **13**: 99–108.
Zhang D., Zhang J., Liu D., Zhao F., Wang H. & Li X. 2016. Inverse conjugate heat conduction and naturalconvection inside an enclosure with multiple unknown wall heating fluxes. *International Journal Heat Mass Transfer* **96**: 312–329.
Zhang W., Zhang C. & Xi G. 2011. Conjugate conduction-natural convection in an enclosure with time-periodic sidewall temperature and inclination. *International Journal Heat Fluid Flow* **32**: 52–64.

[1]*Department of Electrical Enginering*
Faculty of Science and Technology
Universitas Islam Negeri Sultan Syarif Kasim (UIN SUSKA)
28293 Pekanbaru, Riau
INDONESIA
E-mail: marhama.jelita@uin-suska.ac.id, sutoyo@uin-suska.ac.id

[2]*Department of Mathematics*
University of Riau
28293 Pekanbaru, Riau
INDONESIA
E-mail: dr.habibissaleh@gmail.com[*]

[*]Corresponding author